Calculation of flexoelectric coefficients for a nematic liquid crystal by atomistic simulation

David L. Cheung, Stewart J. Clark, and Mark R. Wilson

Citation: J. Chem. Phys. **121**, 9131 (2004); doi: 10.1063/1.1802231
View online: http://dx.doi.org/10.1063/1.1802231
View Table of Contents: http://jcp.aip.org/resource/1/JCPSA6/v121/i18
Published by the American Institute of Physics.

Calculation of flexoelectric coefficients for a nematic liquid crystal by atomistic simulation

David L. Cheung
Department of Chemistry, University of Durham, South Road, Durham DH1 3LE, United Kingdom and Department of Physics, University of Durham, South Road, Durham DH1 3LE, United Kingdom

Stewart J. Clark
Department of Physics, University of Durham, South Road, Durham DH1 3LE, United Kingdom

Mark R. Wilson
Department of Chemistry, University of Durham, South Road, Durham DH1 3LE, United Kingdom

(Received 21 May 2004; accepted 9 August 2004)

Equilibrium molecular dynamics calculations have been performed for the liquid crystal molecule *n*-4-(*trans*-4-n-pentylcyclohexyl)benzonitrile (PCH5) using a fully atomistic model. Simulation data have been obtained for a series of temperatures in the nematic phase. The simulation data have been used to calculate the flexoelectric coefficients e_s and e_b using the linear response formalism of Osipov and Nemtsov [M. A. Osipov and V. B. Nemtsov, Sov. Phys. Crstallogr. **31**, 125 (1986)]. The temperature and order parameter dependence of e_s and e_b are examined, as are separate contributions from different intermolecular interactions. Values of e_s and e_b calculated from simulation are consistent with those found from experiment. © *2004 American Institute of Physics.* [DOI: 10.1063/1.1802231]

I. INTRODUCTION

Atomistic computer simulation provides a powerful tool for the investigation of the properties of soft condensed matter systems. Of particular interest has been the progress made in the simulation of complicated self-ordering systems such as liquid crystal phases.[1–6] Here changes in molecular alignmnent can occur on relatively long times scales (>1 ns) and accurate force fields are required for simulations to reproduce the stability of the phases.[7–10] In principle the bulk material properties of a system should be available from accurate atomistic simulations.[11] However, calculation of the physical properties of mesogenic systems in this way is a challenging task. In this paper we use atomistic simulations to study the flexoelectric effect and calculate the flexoelectric coefficients of the nematic liquid crystal *n*-4-(*trans*-4-n-pentylcyclohexyl)benzonitrile (PCH5, Fig. 1).

The *flexoelectric effect*[12,13] describes the spontaneous polarization generated by a deformation of the director in a nematic phase composed of molecules, which exhibit shape asymmetry and have permanent dipole moments. A system of wedge-shaped molecules with longitudinal dipoles will exhibit a polarization when the director field is subjected to a splay deformation, as shown in Fig. 2(a). Likewise a system of banana-shaped molecules with transverse dipoles will exhibit a polarization under bend as shown in Fig. 2(b). For rod-shaped polar molecules, such as PCH5, flexoelectric polarization is expected to result from the effect of splay and bend deformations on transcient dipole dimers of these molecules. Highly polar mesogens such as PCH5 often associate with antiparallel alignment between dipoles.[14,15] When these dimers are subjected to a splay or bend deformation the dipoles are no longer antiparallel leading to a net polarization, as shown in the top illustration in Fig. 3. The flexoelectric effect can also be present in quadrupolar mesogens.[16] This can arise due to a change in the quadrupole density when the director is splayed, as shown in the bottom illustration in Fig. 3. PCH5 is known also to exhibit strong quadrupolar interactions.[17] However, the extent to which this mechanism contributes to the flexoelectric effect in systems of rod-shaped molecules such as PCH5 is unknown.

In all cases, a phenomological expression for the flexoelectric polarization per unit volume is given by[18]

$$\mathbf{p}^f = e_s \mathbf{n}(\nabla \cdot \mathbf{n}) + e_b \mathbf{n} \times \nabla \times \mathbf{n}, \tag{1}$$

where e_s and e_b are the splay and bend flexoelectric coefficients. The flexoelectric coefficients appear also in the free energy density of a nematic liquid crystal.[19] Here they describe the coupling between director deformations and an applied electric field. This is the converse flexoelectric effect where an applied electric field can distort the director field.[12]

The flexoelectric effect has a large influence on many phenomena in liquid crystals.[20] Technologically it plays a key role in some device applications. Flexoelectric surface switching is important in newly developed bistable displays.[21,22] Flexoelectric coupling in chiral and twisted nematic crystals[23] leads to a linear rotation of the optic axis and also leads to device applications.[24] Flexoelectric coupling in smectic liquid crystals has been shown to stabilize helical structures.[25] The flexoelectric effect is present also in lipid membranes.[26] The direct link between molecular structure and the flexoelectric effect also makes it of fundamental interest.

There have been several experimental studies of the flexoelectric effect (see Refs. 27 and 28 and references therein). However, e_s and e_b are difficult to determine from experiment. Several theoretical studies have also been

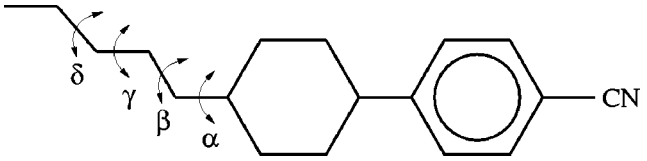

FIG. 1. Structure of PCH5 showing dihedral angles α, β, γ, and δ.

performed[29–36] to study the role of molecular structure in determining flexoelectric behavior. These include an Onsager-like theory,[29] a mean-field theory (including attractive and repulsive interactions),[30] and density functional theories.[33,34] By necessity numerical results from these theories have only been determined for simple models of liquid crystals. Recently more sophisticated theoretical studies have attempted to calculate the flexoelectric coefficients using more realistic models of liquid crystals[35] or to take the effect of intermolecular interactions into account.[36]

There have only been three simulation studies of the flexoelectric effect.[37–40] Two of these used simple models of wedge-shaped liquid crystal molecules formed by fusing a Gay-Berne molecule and a Lennard-Jones molecule. The first of these studies[37,38] used a density functional approach based on Ref. 29 while the second used a linear-response formalism.[32] Qualitatively these studies gave similar results. The bend coefficient was found to be negligible, in line with Meyer's predictions based on molecular shape.[12] However, the values for e_s differed by an order of magnitude. This difference is due to the approximations made in calculating the direct correlation function in the density functional method. Previous studies of the nematic elastic constants[41–43] have shown that approximations made in calculating the direct correlation function can lead to large errors in the values of the elastic constants. Another study[40] compared flexoelectric coefficients calculated from an atomistic simulation to theoretical calculations. Again this used density functional theory (DFT) and an approximate direct correlation function, although reasonable agreement between simulation and experimental values of the flexoelectric coefficients was reported.

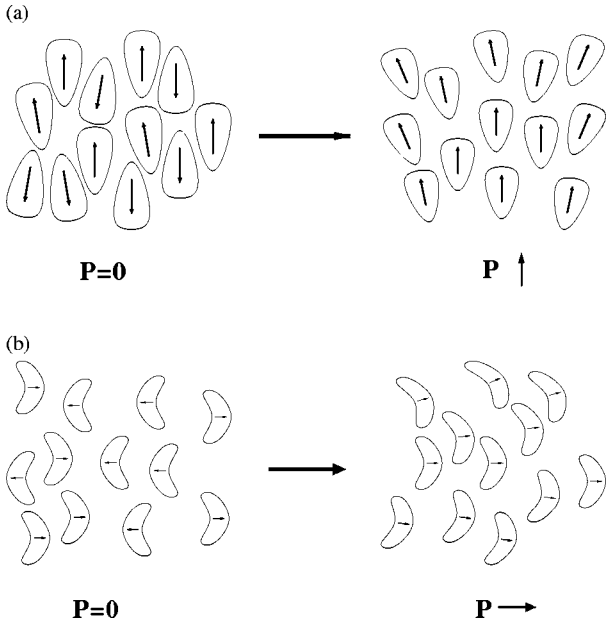

FIG. 2. Polarization in a nematic composed of (a) wedge-shaped molecules with longitudinal dipoles. (b) banana-shaped molecules with transverse dipoles.

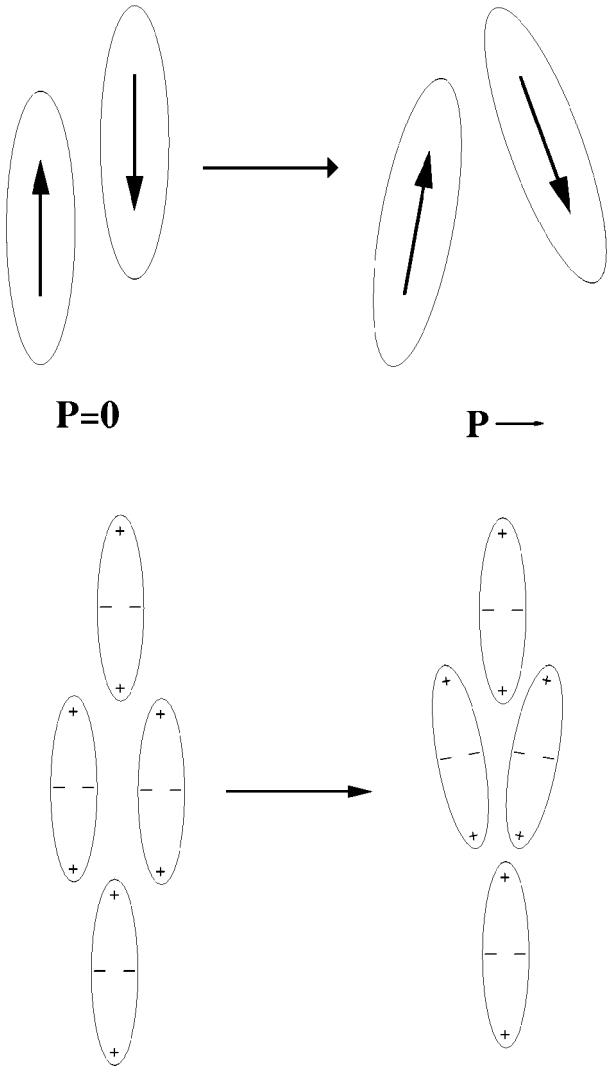

FIG. 3. Microscopic mechanism for flexoelectricity in top: symmetric polar liquid crystals; bottom: quadrupolar mesogens.

II. THEORY

In this work we turn to the linear-response formalism of Osipov and Nemtsov[32] as a means of calculating flexoelectric coefficients. e_s and e_b are related to the response function of the system to an orientational stress. Specifically the polarization is given by

$$P_\alpha = E_{\alpha\beta\gamma}\gamma_{\beta\gamma}, \tag{2}$$

where $\gamma_{\alpha\beta}$ is the deformation tensor given by

$$\gamma_{\alpha\beta} = \frac{\partial \theta_\alpha}{\partial r_\beta}, \tag{3}$$

where θ is the rotation of the director about the axis given by α. For small deformations this is

TABLE I. Equilibrium bond lengths.

Bond	l_{eq} (Å)
CA-CA	1.380
CA-HA	1.080
CA-Cn	1.498
CA-CZ	1.410
Cn-Cn	1.511
Cn-HC	1.088
CZ-NZ	1.173

TABLE II. Bond angle bending parameters.

Angle	k_θ (kcal mol^{-1} rad^{-2})	θ_0 (deg)
CA-CA-CA	280.00	120.0
CA-CA-HA	74.56	120.0
CA-CA-CZ	101.40	120.0
CA-CA-Cn	140.00	120.0
CA-Cn-Cn	126.00	114.0
CA-Cn-HC	70.00	109.5
Cn-Cn-Cn	116.70	112.7
Cn-Cn-HC	88.54	110.7
HC-Cn-HC	66.00	107.8
CA-CZ-NZ	53.80	180.0

$$\gamma_{\alpha\beta}=\epsilon_{\alpha\mu\nu}n_\mu\partial_\beta n_\nu \tag{4}$$

with $\partial_\beta n_\nu=\partial n_\nu/\partial r_\beta$ and $\epsilon_{\alpha\beta\gamma}$ is the Levi-Citva tensor. The response function $E_{\alpha\beta\gamma}$ is

$$E_{\alpha\beta\gamma}=-\frac{\beta}{V}\langle P_\alpha\Pi_{\beta\gamma}\rangle, \tag{5}$$

where **P** is the polarization and

$$\Pi_{\alpha\beta}=-\frac{1}{2}\sum_{i\neq j} r_{ij\alpha}\tau_{ij\beta}. \tag{6}$$

Here $\mathbf{r}_{ij}$ is the intermolecular vector between i and j and τ_{ij} is the torque exerted on i by j.

Explicit expressions for the flexoelectric coefficients can be found by writing $E_{\alpha\beta\gamma}$ as

$$E_{\alpha\beta\gamma}=E_1\epsilon_{\alpha\beta\gamma}+E_2\epsilon_{\mu\alpha\beta}n_\mu n_\gamma+E_3\epsilon_{\mu\gamma\beta}n_\mu n_\alpha + E_4\epsilon_{\mu\alpha\gamma}n_\mu n_\beta. \tag{7}$$

Multiplying this by the deformation tensor Eq. (3) gives

$$P_\alpha=(E_3-E_1)n_\alpha\partial_\gamma n_\gamma-(E_1+E_2)n_\gamma\partial_\gamma n_\alpha. \tag{8}$$

An expression for e_s can then be found by multiplying Eq. (7) by $\epsilon_{\mu\beta\gamma}n_\mu n_\alpha$ and an expression for e_b can be found by multiplying Eq. (7) by $\epsilon_{\mu\alpha\beta}n_\mu n_\gamma$. Doing this gives

$$e_s=-\tfrac{1}{2}E_{\alpha\beta\gamma}\epsilon_{\mu\beta\gamma}n_\mu n_\alpha \tag{9}$$

and

$$e_b=-\tfrac{1}{2}E_{\alpha\beta\gamma}\epsilon_{\mu\alpha\beta}n_\mu n_\gamma. \tag{10}$$

For the purposes of simulation it is convenient to put this in a director based frame of reference. With $\mathbf{n}=\hat{\mathbf{z}}$ Eqs. (9) and (10) become

$$e_s=-\tfrac{1}{2}(E_{zxy}-E_{zyx}), \tag{11}$$

$$e_b=-\tfrac{1}{2}(E_{xyz}-E_{yxz}). \tag{12}$$

III. SIMULATION MODEL AND METHODOLOGY

PCH5 molecules (Fig. 1) were represented using a harmonic all-atom force field of the AMBER form.[44] The force field parameters were taken from our earlier work[7] and are shown in Tables I, II, III, and IV. In Ref. 7 the force field parameters are obtained by fitting to a combination of high-level density functional theory calculations for the intramolecular parts of the potential and molecular dynamics simulations (to obtain liquid densities and heats of vaporization) for the intramolecular parts of the potential.

Molecular dynamics simulations were performed using the DL_POLY program version 2.12.[45] The equations of motion were integrated using the leapfrog algorithm with a time step of 2 fs. Bond lengths were constrained using the SHAKE algorithm.[46] Simulations were performed in the NpT ensemble using the Nosé-Hoover thermostat and barostat[47–49] with relaxation times of 1 ps and 4 ps, respectively. Long range electrostatic interactions were evaluated using an Ewald sum with a convergence parameter of 0.24 Å^{-1} and 11 wave vectors in the x, y, and z directions.

The simulations were started from a cubic system of 216 molecules at a gas phase density. The initial state was a highly ordered nematic ($\overline{P_2}\approx 0.9$) with antiferroelectric ordering. This was then rapidly compressed to a liquid state density (about 500–1000 kg m^{-3}). An equilibration run of $\approx$1 ns was then performed after which statistics were then gathered over 4 ns at each temperature (300, 310, 320, and 330 K). Coordinate data for the calculation of the flexoelectric coefficients were saved every 500 time steps (1 ps).

IV. CALCULATION OF e_s AND e_b

The response function $E_{\alpha\beta\gamma}$ was calculated for each set of saved coordinate data. The polarization **p** was calculated from

$$\mathbf{p}=\sum_i q_i\mathbf{r}_i, \tag{13}$$

where q_i are the atomic charges and $\mathbf{r}_i$ are the atomic position vectors. The sum in Eq. (13) runs over all the atoms in the simulation.

The orientational stress tensor is calculated from the torques and center-of-mass positions of the molecules. The torque on molecule i from molecule j, τ_{ij}, is found from

$$\tau_{ij}=\sum_k \mathbf{r}_\kappa^c\times\mathbf{F}_{kj}, \tag{14}$$

TABLE III. Dihedral angle force constants. All values in kcal mol^{-1}.

Dihedral	V_1	V_2	V_3	V_4	V_5	V_6
CA-CA-CA-CA	0.0	9.51	0.0	0.0	0.0	0.0
CA-CA-Cn-Cn	0.0	0.525	0.0	−0.233	0.0	−0.046
CA-Cn-Cn-Cn	0.0	0.0	0.462	0.0	0.0	0.0
Cn-Cn-Cn-Cn	1.957	0.074	0.028	−0.376	0.039	0.014
Cn-Cn-Cn-HC	0.0	0.0	0.366	0.0	0.0	0.0
HC-Cn-Cn-HC	0.0	0.0	0.318	0.0	0.0	0.0

where $\mathbf{r}_k^c$ is the position vector of atom k in i relative to the center of mass of molecule i, $\mathbf{F}_{kj}$ is the force on k from molecule j and the sum runs over all atoms in i. $\mathbf{F}_{kj}$ is given by

$$\mathbf{F}_{kj}=\sum_l \mathbf{F}_{lk}, \tag{15}$$

where $\mathbf{F}_{lk}$ is the force on atom k from atom l in molecule j and the sum runs over all the atoms in molecule j. The force between two atoms is the sum of the van der Waals force and the electrostatic force. The van der Waals force is of the Lennard-Jones form

$$\mathbf{F}_{kl}^{vdw}=24\epsilon_{kl}\left[\frac{2\sigma_{kl}^{12}}{r_{kl}^{13}}-\frac{\sigma_{kl}^{6}}{r_{kl}^{7}}\right]\hat{\mathbf{r}}_{kl}, \tag{16}$$

where ϵ_{kl} and σ_{kl} are the usual van der Waals parameters and $\hat{\mathbf{r}}_{kl}$ is the unit vector along the direction between k and l. As the van der Waals interaction is short ranged this is only evaluated for pairs of atoms less than 12 Å apart, in common with the forces calculated in the simulation.

The electrostatic force was evaluated using Coulomb's law

$$\mathbf{F}_{kl}^{elec}=\frac{1}{4\pi\epsilon_0}\frac{q_k q_l}{r_{kl}^2}\hat{\mathbf{r}}_{kl}. \tag{17}$$

Due to the long-range of the electrostatic interaction this is calculated for all pairs of atoms in the system (or their minimum image separations). For our system containing 9504 atoms there are ≈45 million atom pairs so this is a large computational task.

TABLE IV. Nonbonded interaction parameters.

Atom	ϵ (kcal mol^{-1})	σ (Å)	q/e
CA	0.070	3.550	−0.122
CA (bridging)	0.070	3.550	0.0
CA (CA-CZ)	0.070	3.550	+0.035
CA (CA-Cn)	0.070	3.550	0.0
CZ	0.150	3.650	+0.395
Cn (CH_3)	0.066	3.500	−0.180
Cn (CH_2)	0.066	3.500	−0.120
Cn (CH)	0.066	3.500	−0.060
HA	0.030	2.420	+0.122
HC	0.030	2.500	+0.060

V. RESULTS

A. Densities and order parameters

Simulation volumes and calculated densities are shown in Table V. As can be seen there is good agreement between calculated densities and the experimental values[50] (better than 5% in each case). Shown in Table VI are the values of the order parameter $\overline{P_2}$ calculated from simulation. These were calculated using two different methods. In the first method, the molecular long axis was obtained by diagonalizing the inertia tensor

$$I_{\alpha\beta}=\sum_{i=1}^{n} m_i(r_i^2\delta_{\alpha\beta}-r_{i\alpha}r_{i\beta}). \tag{18}$$

Here $\mathbf{r}_i$ is the position vector of the ith atom relative to the molecular center of mass and the sum runs over all atoms in the molecule. In the second method, the molecular axis is obtained from the dipole axis. In both cases the director and order parameter are found by diagonalizing the ordering tensor

$$Q_{\alpha\beta}=\sum_{i=1}^{N}\frac{3}{2}u_{i\alpha}u_{i\beta}-\frac{1}{2}\delta_{\alpha\beta}, \tag{19}$$

where $\mathbf{u}_i$ is the molecular long axis, found from the molecular long axis or the molecular dipole axis. The sum in Eq. (19) runs over all molecules in the simulation. Also shown in Table VI are the experimental order parameters found from Raman scattering.[51] The simulated order parameters found from the inertia tensor are slightly higher than the experimental values at all three temperatures in the nematic phase but are nonetheless in quite good agreement with experiment. For the highest temperature studied (330 K) the simulated system remains nematic, which suggests that either some super heating of the nematic phase is occuring in the simulation, or that a combination of system size effects and inaccuracies in the force field mean that we are not able to predict the phase transition (328 K) exactly. Both are likely explanations. Simulations of single site potentials (where

TABLE V. Computed densities for simulation PCH5.

T (K)	V (Å^3)	$\langle\rho\rangle$ (kg m^{-3})	$\rho_{expt.}$ (kg m^{-3})
300	92468±688.4	997.5±7.4	963.0
310	92912±745.8	992.9±8.0	956.5
320	94033±777.5	981.1±8.1	949.6
330	94824±761.1	972.9±10.0	⋯

TABLE VI. Orientational order parameter $\overline{P}_2$ of PCH5 calculated from simulation.

T (K)	$\overline{P}_2^{inertia}$	$\overline{P}_2^{dipole}$	$\overline{P}_2^{expt.}$
300	0.68±0.02	0.45±0.01	0.63
310	0.65±0.01	0.47±0.00	0.58
320	0.55±0.03	0.39±0.01	0.50
330	0.51±0.04	0.36±0.02	0.00

longer simulation runs are possible) point to some hystersis in cooling/heating through the phase transition, particularly with small system sizes. The most detailed atomistic study of the nematic-isotropic transition conducted top date, for the first three homologs of the phenylalkyl-4-(4′ cyanobenzylidene)-aminocinnamates, was able to predict transitions temperatures to within 10 ± 5 K.[4]

The order parameters found from the dipole moment are significantly lower than those found from the inertia tensor as well as being lower than the Raman scattering results for temperatures below $T_{NI}^{\text{expt.}}$. Here the partial charges on the hydrogens in the tail (which is less aligned than the ring systems) have a significant influence on the overall order parameter. We therefore expect the calculated dipolar order parameter to be smaller than the Raman results, where the chromophores (C-N bond and symmeteric phenyl stretch) are better ordered.

The translational order of the system can be studied through the center of mass radial distribution function (RDF), $g(r)$, and the RDF resolved parallel to the director $g_{\parallel}(r)$. These are shown in Fig. 4. As can be seen $g(r)$ shows a first solvation peak at ≈ 6 Å, consistent with a fluid phase and $g_{\parallel}(r)$ remains flat showing no periodic ordering of molecules. Hence, the simulated liquid crystal phase is nematic and no trace of smectic ordering is seen.

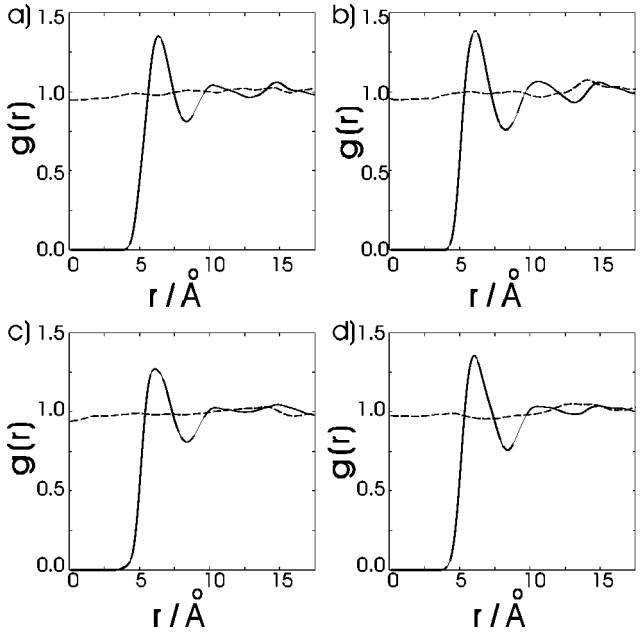

FIG. 4. Radial distribution functions for simulated PCH5 at (a) 300 K, (b) 310 K, (c) 320 K, and (d) 330 K. The solid line shows the radial distribution function and the dashed line shows the radial distribution function resolved parallel to the director.

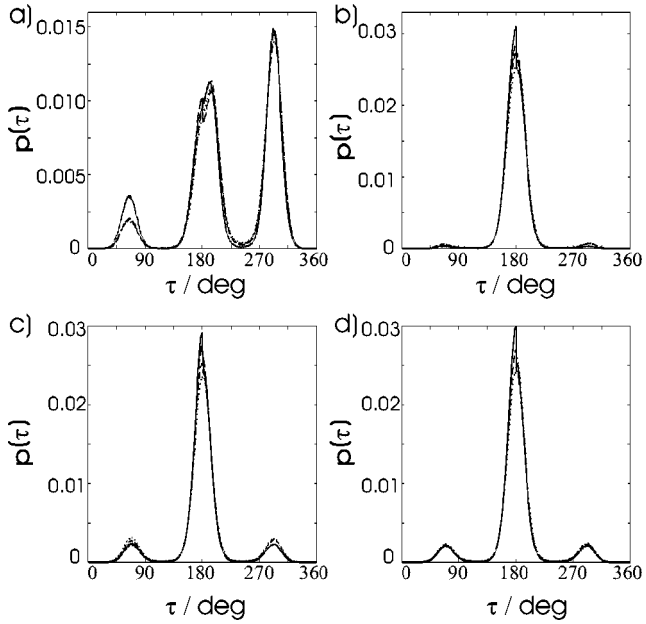

FIG. 5. Dihedral angle distribution functions for the alkyl tail of PCH5. In each graph the solid line indicates the data for 300 K, the long dashed line indicates the data at 310 K, the short dashed line indicates the data at 320 K, and the dotted line shows the data at 330 K.

B. Molecular structure

Shown in Fig. 5 are the dihedral distribution functions for some of the dihedrals in the alkyl tail, as shown in Fig. 1. These have an important effect on the overall shape of the molecule. The percentage of dihedrals in the *trans* and *gauche* states can be calculated by integrating over these distributions and these are shown in Table VII. The *gauche* populations increase with temperature as would be expected. The largest *gauche* populations occur for the γ dihedral. This

TABLE VII. Dihedral angle populations for simulated PCH5. (a) Dihedral angle β, (b) dihedral angle γ, and (c) dihedral angle δ.

	(a) β		
T (K)	*trans*	*gauche*−	*gauche*+
300	97.5%	1.2%	1.3%
310	97.7%	1.2%	1.1%
320	95.5%	2.3%	2.2%
330	95.4%	2.0%	2.6%
	(b) γ		
300	85.3%	7.4%	7.3%
310	85.5%	7.2%	7.3%
320	81.8%	8.9%	9.3%
330	79.9%	10.1%	10.0%
	(c) δ		
300	86.7%	6.7%	6.6%
310	86.4%	6.9%	6.7%
320	85.3%	7.2%	7.5%
330	84.5%	7.6%	7.9%

TABLE VIII. Principal moments of inertia and axes lengths of the equivalent inertia spheroid.

T (K)	I_{aa} ($\times 10^{-45}$ kg m^2)	I_{aa} ($\times 10^{-45}$ kg m^2)	I_{aa} ($\times 10^{-45}$ kg m^2)	$2a$ (Å)	$2b$ (Å)	$2c$ (Å)
300	5.197±0.034	84.394±0.139	86.083±0.132	19.74	4.03	2.88
310	5.172±0.004	84.312±0.022	85.985±0.021	19.74	4.02	2.87
320	5.290±0.028	83.900±0.186	85.896±0.166	19.68	4.07	2.89
330	5.315±0.024	83.786±0.024	85.557±0.078	19.67	4.09	2.89

is consistent with previous studies[2,3] and predictions of mean field theory.[52] States where the tail is linear, such as the all *trans* state and states with γ in a *gauche* state and β and δ *trans*, are of lower energy (and hence of higher probability) than states where the tail is nonlinear. The *trans* populations in the alkyl tail are larger than those for organic liquids such as butane or hexane.[7] As butane and hexane are isotropic liquids the dihedral populations are not subject to an ordering mean field.

The molecular shape can also be approximately characterized by the equivalent inertia spheroid.[2] This is a spheroid with an uniform mass density and the same total mass M as the molecule. The dimensions of this give an approximate measure of molecular length, breadth, and width. These are found from the principal moments of inertia I_{aa}, I_{bb}, and I_{cc}, i.e., the eigenvalues of the inertia tensor Eq. (18). The lengths of each of the axes $2a$, $2b$, and $2c$ are given by

$$a=\sqrt{\frac{2.5(I_{bb}+I_{cc}-I_{aa})}{M}},$$
$$b=\sqrt{\frac{2.5(I_{cc}+I_{aa}-I_{bb})}{M}}, \tag{20}$$
$$c=\sqrt{\frac{2.5(I_{aa}+I_{bb}-I_{cc})}{M}}.$$

Shown in Table VIII are the principal moments of inertia and the equivalent axes lengths for simulated PCH5. The molecular length $2a$ shows a slight decrease with temperature, while the molecular breadth and width show a slight increase. This is expected from the dihedral angle distributions and shows that the molecule becomes longer and thinner as the system goes further into the nematic phase. This is in accordance with mean-field theory as discussed above. The ratio between c and b is roughly 0.71 across the temperature range studied. These results are similar to those obtained in a previous atomistic simulation of *trans*-4-(*trans*-4-n-pentylcyclohexyl)cyclohexylcarbonitrile (CCH5)[2] where there was a slight change in the axis lengths with temperature within the nematic phase and a larger change on going into the isotropic phase.

C. Polarization

The polarization was calculated from the atomic charges and positions using Eq. (13) for each set of coordinate data and the average polarizations are shown in Table IX. The time evolution of the polarization at each temperature is shown in Fig. 6. As can be seen at each temperature there is a small net polarization, particularly directed along the director. This is a consequence of the finite system size and short simulation lengths (about 1 ns compared to a time scale of 10–100 ns for molecular reorientation) rather than any intrinisic polar ordering.

The reorientational motion of the molecules can be investigated using the reorientational time-correlation functions[53,54]

$$C_l(t)=\langle P_l(\hat{\mathbf{u}}_i(t_0)\cdot\hat{\mathbf{u}}_i(t_0+t))\rangle, \tag{21}$$

where $\hat{\mathbf{u}}_i$ is a unit vector defining the orientation of the molecule and $P_l(x)$ is the lth Legendre polynomial. $C_l(t)$ for this is shown in Fig. 7. The decay of $C_1(t)$ is slow at all temperatures. This reflects the long times needed for a molecule in the nematic phase to rotate its long axis. This is the reason for the freezing in of a net polarization in this system. All the $C_l(t)$ are similar to those found for other liquid crystal systems[3] and qualitatively similar to those obtained for simple liquids[53,55] but with a longer decay time.

To ensure that there is no long-range polar order in the system, the simulation data has been used to calculated the orientational correlation functions $g_1(r)$ and $g_2(r)$. These are shown in Fig. 8. As can be seen after an initial minima, $g_1(r)$ oscillates about 0. In contrast $g_2(r)$ has a maxima at about 5 Å, which is then followed by a decay to a value of about $\overline{P_2^2}$. The average values of the polarization are shown in Table IX.

D. Flexoelectric coefficients

The flexoelectric coefficients have been calculated using Eqs. (9) and (10) and are shown in Table X. Experimental data for e_s and e_b in a nematic is scarce and often ambiguous[28] and in many cases there is considerable contro-

TABLE IX. Computed system polarizations. Here the director lies along the z axis and $|\mathbf{p}|$ is the magnitude of the polarization vector $\mathbf{p}$.

T (K)	p_x ($\times 10^{-30}$ C m)	p_y ($\times 10^{-30}$ C m)	p_z ($\times 10^{-30}$ C m)	$\lvert\mathbf{p}\rvert$ ($\times 10^{-30}$ C m)
300	3.12±4.63	−17.32±2.65	15.46±1.33	23.92±2.58
310	3.24±2.51	−10.06±2.71	19.54±1.38	22.48±1.94
320	2.22±4.03	1.14±4.53	14.07±1.62	15.51±1.72
330	1.10±3.83	−0.52±3.55	4.74±2.00	7.12±2.14

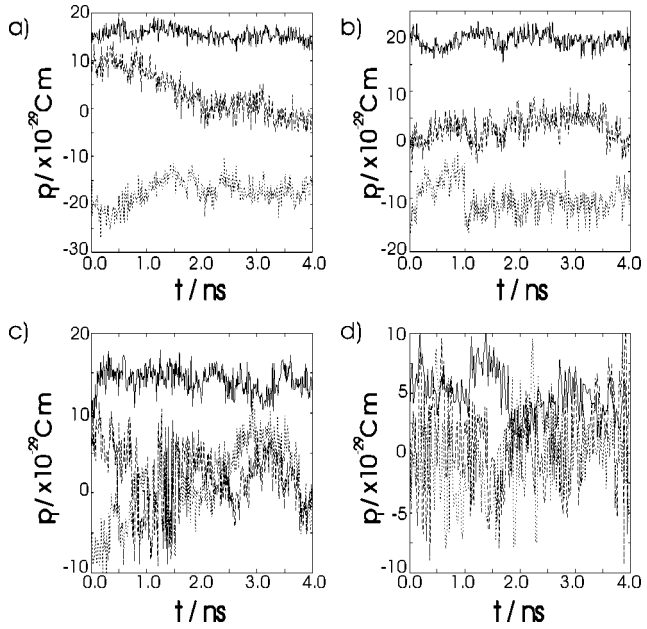

FIG. 6. System polarization against time for simulated PCH5 at (a) 300 K, (b) 310 K, (c) 320 K, and (d) 330 K. The solid line denotes the polarization parallel to the director, while the dashed and dotted lines show the polarization perpendicular to the director.

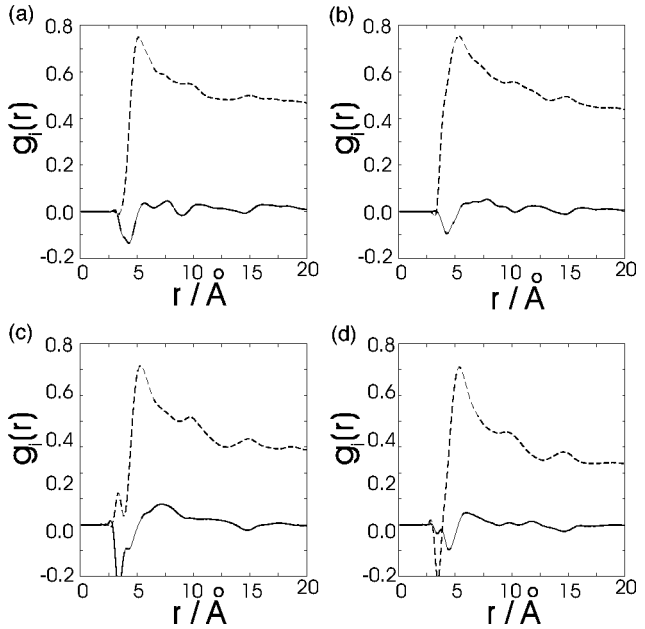

FIG. 8. Orientational correlation functions $g_1(r)$ (solid line) and $g_2(r)$ (dashed line) at (a) 300 K, (b) 310 K, (c) 320 K, and (d) 330 K.

versy over the sign of the flexoelectric coefficients. Generally the absolute values for e_s and e_b are of the order of $10\,\mathrm{pC\,m^{-1}}$, which is the same order of magnitude as the results presented here. For PCH5, experimental values for the flexoelectric coefficients have been determined[27] with e_s given as $5.3\,\mathrm{pC\,m^{-1}}$ and e_b as $3.3\,\mathrm{pC\,m^{-1}}$ at 303 K, with quoted errors of about 40%. The temperature dependence of e_s and e_b was not fully considered in that study, the normalized difference of the coefficients $(e_s-e_b)/k_2$, where k_2 is the twist elastic constant, was measured and found to remain constant across the nematic range.

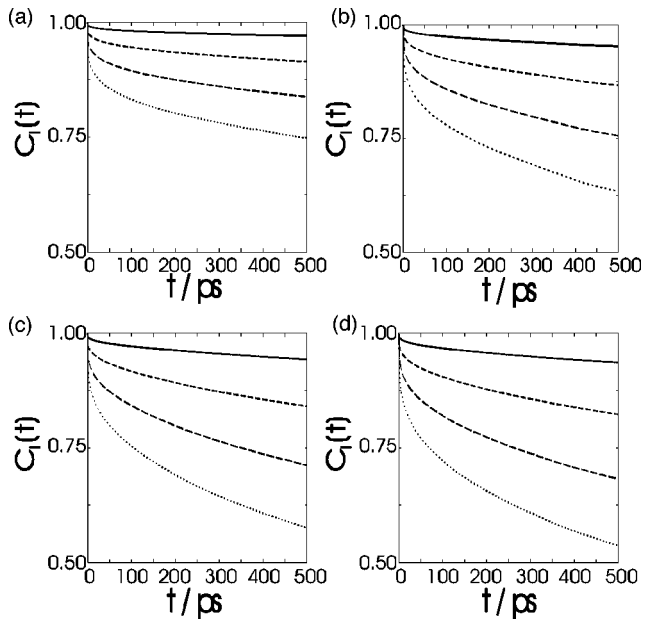

FIG. 7. Orientational time correlation functions $C_l(t)$ $(l=1,2,3,4)$ for simulated PCH5 calculated using the molecular long axis found from the inertia tensor (3.52). (a) 300 K, (b) 310 K, (c) 320 K, and (d) 330 K. In each graph $C_1(t)$ is shown by the solid line, $C_2(t)$ is shown by the short dashed line, $C_3(t)$ is shown by the long dashed line, and $C_4(t)$ is shown by the dotted line.

The errors for the individual flexoelectric coefficients in Table X are quite large but several features can be noted from the results. The sign of both e_s and e_b are positive throughout, with the splay coefficent slightly larger for most temperatures and, within experimental error, the value of the flexoelectric coefficients drop with increasing temperature. This behavior could be rationalized in a number of ways. PCH5 is known to form transcient dipole dimers in both the nematic phase and the pretransitional region of the isotropic phase.[15,56] Increases in temperature are likely to reduce the strength of the interactions between the transcient dimers and reduce the dipolar coupling between molecules, thereby reducing the flexoelectric effect. It is interesting to note that temperature is likely also to effect the mean molecular dipole moment. As the temperature increases the probability of the tail adopting a *gauche* conformation increases. The increase in the *gauche* populations with temperature can be seen from Fig. 5 and Table VII. This could cause the molecule to become increasingly bow shaped decreasing the longitudinal dipole moment and increasing the transverse dipole moment. The dipole moment of molecule i, $\mathbf{m}_i$, and its longitudinal and transverse components $\mathbf{m}_{li}$ and $\mathbf{m}_{ti}$ are given by

TABLE X. Calculated flexoelectric coefficients for simulated PCH5.

T (K)	e_s ($\mathrm{pC\,m^{-1}}$)	e_b ($\mathrm{pC\,m^{-1}}$)
300	45.9 ± 30.8	51.2 ± 11.1
310	80.7 ± 15.6	16.5 ± 7.5
320	34.8 ± 11.0	6.2 ± 5.5
330	11.1 ± 2.9	8.8 ± 0.3

TABLE XI. Average dipole moments per molecule calculated using Eqs. (22), (23), and (24).

T (K)	$\langle\lvert\mathbf{m}\rvert\rangle$ ($\times 10^{-30}$ C m)	$\langle\lvert\mathbf{m}_l\rvert\rangle$ ($\times 10^{-30}$ C m)	$\langle\lvert\mathbf{m}_t\rvert\rangle$ ($\times 10^{-30}$ C m)
300	6.47±0.52	3.35±1.94	4.97±1.58
310	6.46±0.53	3.30±1.89	5.02±1.55
320	6.47±0.54	3.13±1.83	5.19±1.42
330	6.47±0.54	3.18±1.87	5.14±1.47

$$\mathbf{m}_i = \sum_j q_j \mathbf{r}_j , \tag{22}$$

$$\mathbf{m}_{li} = (\mathbf{m}_i \cdot \hat{\mathbf{u}}_i)\hat{\mathbf{u}}_i , \tag{23}$$

$$\mathbf{m}_{ti} = \mathbf{m}_i - (\mathbf{m}_i \cdot \hat{\mathbf{u}}_i)\hat{\mathbf{u}}_i , \tag{24}$$

where q_j is the charge on atom j, $\mathbf{r}_j$ is the position vector of atom j, and $\hat{\mathbf{u}}_i$ is the molecular long axis found from diagonalizing the inertia tensor. The sum in Eq. (22) runs over all atoms in molecule i. The average molecular dipoles have been calculated and are shown in Table XI. The average longitudinal dipole moment decreases between 300 K and 320 K, and the transverse dipole moment shows a corresponding increase. The reduction in $\mathbf{m}_{li}$ would again reduce the strength of the dipolar coupling between pairs of molecules and as a consequence would reduce the flexoelectric coefficients if the mechanism for flexoelectricity involved a disruption of dipolar coupling (top illustration in Fig. 3).

The temperature dependence of e_s and e_b calculated here can be compared with the temperature dependence predicted theoretically. One such study[36] calculated e_s and e_b for the mesogen 4′-n-pentyl-4-cyanobiphenyl (5CB), similar in structure to PCH5, with a density functional approach. The molecules were modeled using a dipolar Gay-Berne potential[57] and the direct correlation function was calculated using a modified Bethe theory[58,59] and the Percus-Yevick closure approximation.[53] This study found e_s and e_b to be constant. The model used, however, neglected both molecular flexibility and long-range dipole-dipole interactions, only interactions between nearest and next nearest neighbors were considered. The flexoelectric coefficients of the mesogen 4′-methoxybenzylidene-4-n-butylaniline (MBBA) have also been calculated using a mean field model.[35] e_s and e_b were both found to decrease monotonically with temperature using this method.

Comparison with previous simulation results[37–39] is possible only on the qualitative level due to the vast differences in the models used. PCH5 is far from the idealized pear-shaped molecules used previously. The simulations of Billeter and Pelcovits, and Zannoni and co-workers found that the splay flexoelectric coefficient decreases with temperature in agreement to the present results.

The dependence of e_s and e_b on the order parameter $\overline{P}_2$ is shown in Fig. 9. The order parameter dependence of e_s and e_b from previous studies give ambiguous conclusions. Early work[60] suggested that for dipolar molecules the flexoelectric coefficients are predicted to vary as $\overline{P}_2^2$, while for quadrupolar molecules the flexoelectric coefficients should vary as $\overline{P}_2$.[16] Using mean-field theory Osipov[30] showed that both $\overline{P}_2$ and $\overline{P}_2^2$ dependence should be seen. However, it was also suggested that the effect of molecular flexibility would introduce a $\overline{P}_2^{-1}$ dependence.[31] From Fig. 9, a linear dependence on $\overline{P}_2^2$ is seen, indicating that the dipolar flexoelectric effect (top illustration in Fig. 3) is likely to be most important in PCH5.

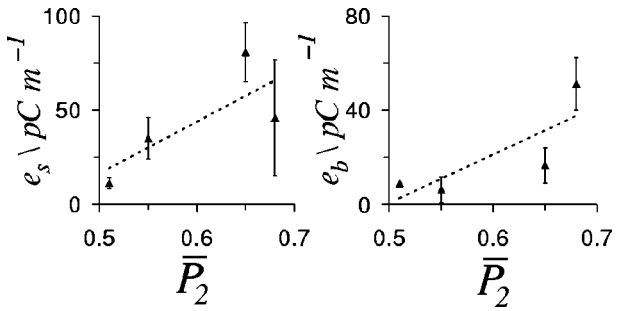

FIG. 9. Order parameter dependence of e_s and e_b. The triangles show the simulated data and dotted lines show linear regression fits to the data.

The contributions from the van der Waals and electrostatic interactions to the flexoelectric coefficients have also been calculated. These are shown in Table XII. The electrostatic contributions to e_s and e_b dominate in each case, as might be expected. It is interesting to note that the sign of van der Waals' contribution to e_s is negative

VI. CONCLUSION

This paper describes the calculation of the flexoelectric coefficients e_s and e_b for a common nematic liquid crystal PCH5 from atomistic simulation. e_s and e_b have been calculated at a range of temperatures in the nematic phase. The temperature and order parameter dependence of e_s and e_b have been examined. Contributions from different intermolecular interactions have been determined also.

The calculated values of e_s and e_b are consistent with values determined from experiment. The splay and bend coefficients are both found to decrease with temperature. This could be explained by a small decrease in the antiparallel dipole correlation in PCH5 as a function of temperature and the small decrease in the longitudinal dipole moment mediated by increases in gauche conformations of the alkyl chain. This would be consistent with a dipolar mechanism for flexoelectricity in PCH5, as would the order parameter dependence of the results. The electrostatic contributions to e_s and e_b are found to dominate the van der Waal's contribution.

The effect of increasing system size on the calculated values of e_s and e_b has not been investigated in this work. This would be of interest but is beyond our current computer capacity. We note that limited simulations of systems of the

TABLE XII. van der Waals and electrostatic contributions to the flexoelectric coefficients (in pC m^{-1}).

T (K)	e_s^{vdw}	e_b^{vdw}	e_s^{elec}	e_b^{elec}
300	−9.8±30.7	15.0±7.7	55.8±4.5	36.2±12.8
310	−4.5±19.2	−0.9±7.7	85.3±5.9	17.4±3.1
320	−10.3±11.7	3.3±2.7	45.1±1.2	2.9±2.9
330	−6.2±2.0	5.0±1.2	17.3±1.0	3.9±1.6

order of 1000 nematogens have recently been performed[56,61] and these do provide a better representation of long-range order. However, studies of such system sizes (44 000 atoms for a fully atomistic model of PCH5) remain extremely computationally expensive at the current time. If the large errors can be reduced through the use of larger system sizes, it may well be possible to use simulation to aid in the design of molecules with larger flexoelectric coefficients.

Extension of this work to different mesogens is possible. Calculation of e_s and e_b for a range of different mesogens would be a good test of the accuracy of the method. It would also be interesting to compare the contributions to e_s and e_b for molecules exhibiting different mechanisms for flexoelectricity, e.g., those exhibiting quadrupolar flexoelectricity. The investigation of alternative routes to e_s and e_b would also be fruitful. Combining the density functional method used in Refs. 37 and 38 with a more accurate method for determining the direct correlation function, such as that recently used by Schmid and co-workers for the calculation of nematic elastic constants[62] could provide an alternative route to the flexoelectric coefficients.

[1] M. R. Wilson, Struct. Bonding (Berlin) **94**, 42 (1999).
[2] M. R. Wilson and M. P. Allen, Liq. Cryst. **12**, 157 (1992).
[3] C. McBride, M. R. Wilson, and J. A. K. Howard, Mol. Phys. **93**, 955 (1998).
[4] R. Berardi, L. Muccioli, and C. Zannoni, ChemPhysChem **5**, 104 (2004).
[5] A. V. Kolmolkin, A. Laaksonen, and A. Maliniak, J. Chem. Phys. **101**, 4103 (1994).
[6] S. Y. Yakovenko, A. A. Muravski, F. Eikelschulte, and A. Geiger, Liq. Cryst. **24**, 657 (1998).
[7] D. L. Cheung, S. J. Clark, and M. R. Wilson, Phys. Rev. E **65**, 051709 (2002).
[8] M. A. Glaser, N. A. Clark, E. Garcia, and C. M. Walba, Spectrochim. Acta, Part A **53**, 1325 (1997).
[9] E. Garcia, M. A. Glaser, N. A. Clark, and D. M. Walba, J. Mol. Struct.: THEOCHEM **464**, 39 (1999).
[10] M. J. Cook and M. R. Wilson, Mol. Cryst. Liq. Cryst. Sci. Technol., Sect. A **357**, 149 (2001).
[11] D. L. Cheung, S. J. Clark, and M. R. Wilson, Chem. Phys. Lett. **356**, 140 (2002).
[12] R. B. Meyer, Phys. Rev. Lett. **22**, 918 (1969).
[13] P. G. de Gennes, *Physics of Liquid Crystals* (Oxford University Press, New York, 1976).
[14] W. Haase, Z. X. Fan, and H. J. Müller, J. Chem. Phys. **89**, 3317 (1988).
[15] M. J. Cook and M. R. Wilson, Liq. Cryst. **27**, 1573 (2000).
[16] J. Prost and J. P. Marcerou, J. Phys. (Paris) **38**, 315 (1977).
[17] M. J. Cook and M. R. Wilson, Liq. Cryst. **27**, 1573 (2000).
[18] P. Rudquist and S. T. Lagerwall, Liq. Cryst. **23**, 503 (1997).
[19] M. P. Allen and A. J. Masters, J. Mater. Chem. **11**, 2678 (2001).
[20] L. M. Blinov and V. G. Chigrinov, *Electrooptic Effects in Liquid Crystals* (Springer, New York, 1993).
[21] C. Denniston and J. Yeomans, Phys. Rev. Lett. **87**, 275505 (2001).
[22] A. J. Davidson and N. J. Mottram, Phys. Rev. E **65**, 051710 (2002).
[23] J. S. Patel and R. B. Meyer, Phys. Rev. Lett. **58**, 1538 (1987).
[24] A. E. Blatch, M. J. Coles, B. Musgrave, and H. J. Coles, Mol. Cryst. Liq. Cryst. **401**, 161 (2003).
[25] M. Čepič and B. Žekš, Phys. Rev. Lett. **87**, 085501 (2001).
[26] A. G. Petrov, Biochim. Biophys. Acta **85535**, 1 (2001).
[27] P. R. M. Murthy, V. A. Raghunathan, and N. V. Madhusudana, Liq. Cryst. **14**, 483 (1993).
[28] A. G. Petrov, *Physical Properties of Liquid Crystals: Nematics*, edited by D. A. Dunmar, A. Fukuda, and G. R. Luckhurst (INSPEC, the Institution of Electrical Engineers, London, 2001), p. 251.
[29] J. P. Stratley, Phys. Rev. A **14**, 1835 (1976).
[30] M. A. Osipov, Sov. Phys. JETP **58**, 1167 (1983).
[31] M. A. Osipov, J. Phys. (France) Lett. **45**, 823 (1984).
[32] M. A. Osipov and V. B. Nemtsov, Sov. Phys. Crystallogr. **31**, 125 (1986).
[33] Y. Singh and U. P. Singh, Phys. Rev. A **39**, 4254 (1989).
[34] A. M. Somoza and P. Tarazona, Mol. Phys. **72**, 911 (1991).
[35] A. Ferrarini, Phys. Rev. E **64**, 021710 (2001).
[36] A. V. Zahkarov and R. Y. Dong, Eur. Phys. J. E **6**, 3 (2001).
[37] J. Stelzer, R. Berardi, and C. Zannoni, Chem. Phys. Lett. **299**, 9 (1999).
[38] J. Stelzer, R. Berardi, and C. Zannoni, Mol. Cryst. Liq. Cryst. Sci. Technol., Sect. A **352**, 186 (2000).
[39] J. L. Billeter and R. A. Pelcovits, Liq. Cryst. **27**, 1151 (2000).
[40] A. V. Zakharov and A. A. Vakulenko, Crystallogr. Rep. **48**, 686 (2003).
[41] J. Stelzer, L. Longa, and H.-R. Trebin, J. Chem. Phys. **103**, 3098 (1995).
[42] J. Stelzer, L. Longa, and H.-R. Trebin, Mol. Cryst. Liq. Cryst. Sci. Technol., Sect. A **262**, 455 (1995).
[43] M. P. Allen, M. A. Warren, M. R. Wilson, A. Sauron, and W. Smith, J. Chem. Phys. **105**, 2850 (1996).
[44] W. D. Cornell, P. Cieplak, C. I. Bayly, I. R. Gould, K. M. Merz, D. M. Ferguson, T. Fox, J. W. Caldwell, and P. A. Kollman, J. Am. Chem. Soc. **117**, 5179 (1995).
[45] DL_POLY is a package of molecular simulation routines written by W. Smith and T. R. Forester, copyright The Council for the Central Laboratory of the Research Councils, Daresbury Laboratory at Daresbury, Nr. Warrington, 1996.
[46] J. P. Ryckaert, G. Ciccotti, and H. J. C. Berensden, J. Comput. Phys. **23**, 327 (1977).
[47] S. Nosé, Mol. Phys. **52**, 1055 (1984).
[48] W. G. Hoover, Phys. Rev. A **31**, 1695 (1985).
[49] S. Melchonnia, G. Ciccotti, and B. L. Holian, Mol. Phys. **78**, 583 (1993).
[50] U. Finkenzeller, T. Geelhaar, G. Weber, and L. Pohl, Liq. Cryst. **5**, 313 (1989).
[51] R. Seeliger, H. Haspeklo, and F. Noack, Mol. Phys. **49**, 1039 (1983).
[52] G. R. Luckhurst, in *Nuclear Magnetic Resonance of Liquid Crystals*, edited by J. W. Emsley (Kluwer, Dordecht, 1985).
[53] J. P. Hansen and I. R. McDonald, *Theory of Simple Liquids*, 2nd ed. (Academic, New York, 1990).
[54] D. J. Tildesley and P. A. Madden, Mol. Phys. **48**, 129 (1983).
[55] M. P. Allen and D. J. Tildesly, *Computer Simulation of Liquids* (Oxford University Press, Oxford, 1989).
[56] M. J. Cook and M. R. Wilson, Mol. Cryst. Liq. Cryst. Sci. Technol., Sect. A **363**, 181 (2001).
[57] J. G. Gay and B. J. Berne, J. Chem. Phys. **74**, 3316 (1981).
[58] A. V. Zakharov, Phys. Rev. E **51**, 5880 (1995).
[59] A. V. Zakharov and S. Romano, Phys. Rev. E **58**, 7428 (1998).
[60] A. Derzhanski and A. G. Petrov, Phys. Lett. A **34**, 483 (1971).
[61] Z. Wang, J. A. Lupo, S. Patnaik, and R. Patcher, Comput. Theor. Polym. Sci. **11**, 375 (2001).
[62] N. H. Phoung, G. Germano, and F. Schmid, J. Chem. Phys. **115**, 7227 (2001).